# Design and Characterisation of Particle Jamming-Based Variable Stiffness Displays using Non-pneumatic Actuators

Joshua Brown and Fernando Bello

Abstract— Particle jamming is an emergent technology widely used to create haptic devices that can change their physical stiffness to render hard or soft surfaces. Conventional implementations of particle jamming-based interfaces have relied on bulky and expensive vacuum systems to force the particles together. This paper presents designs for two alternative, mechatronic approaches to activating a particle jamming-based haptic interface. Each design is subjected to a battery of mechanical tests to evaluate the range and uniformity of the achievable hardness change and response time. Results are presented and the effectiveness of these designs is considered against established pneumatic approaches.

## I. Introduction

Physical hardness, or the resistance to deformation under load, is an important haptic sensation. In medicine, hardness may be the only distinguishing feature between two types of organic tissue, whilst the player of a virtual reality game may wish to feel the difference between walking on soil or stone. Traditionally, force-feedback devices have been used to effectively mimic the sensations experienced when interacting with a soft surface [1].

Recent advances in soft robotics have given rise to new ways of rendering hardness change in haptic interfaces with devices that can become physically harder or softer. Various engineering approaches to building, actuating and controlling such devices have been proposed. However, the vast majority of these have been based on pneumatic actuators.

As effective as these interfaces are, pneumatic approaches to control and actuation are undesirable. Vacuum pumps and air compressors are loud and heavy and not at all suited to the portable and wearable applications promised by soft haptic devices. Moreover, the pneumatic hardware required to control such systems (valves and regulators) are too expensive for consumer devices. There is therefore a need for a non-pneumatic method of actuating such soft haptic devices. This paper focuses on the design and performance of mechanical particle jamming-based tactile displays.

## II. Background

Variable stiffness haptic devices are a well-researched class of haptic interfaces that are able to change their physical stiffness to create a sensation of hardness or softness for their user. These may be based on mechanical [2] or chemical [3] properties of materials, or be the result of a force-feedback simulation of how soft objects and materials behave under load [4], [5].

In recent years, particle jamming has emerged as the favoured method for creating highly controllable variable stiffness displays. A particle jamming-based haptic interface contains a particle fluid (sand, seeds, coffee grounds etc.) contained within a sealed pouch. When the air is evacuated from this fluid, the sides of the pouch compress the particles together, increasing their viscosity [6], [7]. This principle has been used to create tactile devices that can change their hardness and hold their shape [8], as well as devices that can carry haptic vibrations [9], [10], [11] and change their gross [12] and surface [13] shape. Similar stiffness changing effects have been observed when vacuum systems are used to jam layers [14] and fibres [15], in much the same way as particles.

Haptic interfaces based on particle jamming have been used extensively in medical simulation to mimic the feel of soft, organic tissues [16], [17], [18], which can be easily characterised by their physical hardness [19]. Digital sculpting has also been explored, with a novel particle jamming-based modelling surface able to deform whilst being modelled, and then harden in its desired shape [20]. Moreover, the compliance of particle jamming-based devices has seen the techology utilised in wearable interfaces such as haptic gloves [21].

## III. Non-Pneumatic Actuation

Two mechanical approaches to actuating a particle jamming based haptic device have been devised - direct compression (DC) and constrictive actuation (CA). Prototype devices were built using each approach in both touchpad and shaft configurations. The touchpad configuration can be used as a tactile display with the material under the finger changing hardness. The shaft configuration more closely approximates the form and behaviour of a joystick or hand grip (for example a force-feedback handle, VR controller, steering wheel etc).

### A. Direct compression

The direct compression (DC) approach is based on the observation in [10] that a human user interacting with a particle jamming-based haptic device can harden the fluid by compacting it manually. DC therefore works by

The authors are with the Centre for Engagement and Simulation Science (ICCESS), Department of Surgery and Cancer, Imperial College London, UK joshua.brown@imperial.ac.uk, f.bello@imperial.ac.uk

The project was financially supported by Imperial College London under the Digital Innovation Fund

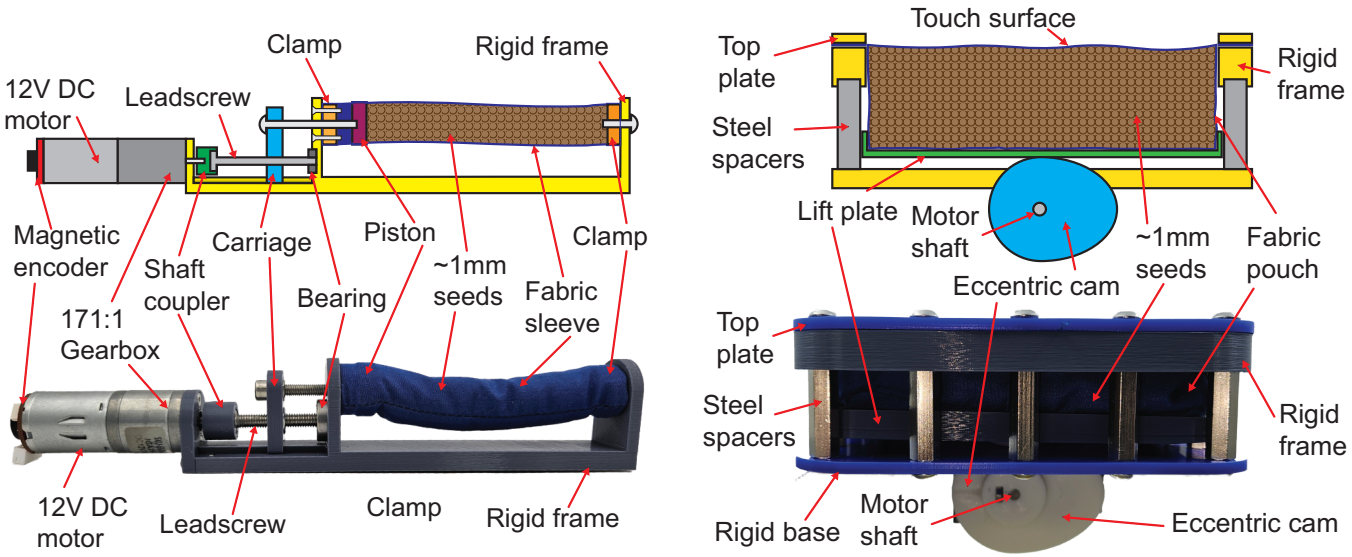


(a) Shaft configuration

(b) Touchpad configuration

Fig. 1: The direct compression technique applied to a) a shaft and b) a touchpad.

exerting a force on the particle fluid, such that it becomes compressed against its soft but inelastic container. The more force that is exerted this way, the more compressed the fluid becomes, increasing stiffness.

1) Shaft configuration: In the shaft configuration, an inelastic fabric sleeve (100 mm L × 20 mm dia.) is filled with a particle fluid (Quinoa seeds of ~1 mm dia). One end is folded over a plastic disc and clamped to a soild plastic frame. A piston is inserted into the other end with another plastic disc, which is again clamped to the plastic frame, such that the fabric sleeve is fixed at both ends but the piston is able to move along the axis of the sleeve. The piston is then driven by a leadscrew, powered by a DC motor. When the piston is driven into the fluid, it compacts and becomes harder. When it recedes, the fluid relaxes and becomes softer. A schematic view of this arrangement and the working prototype are shown in Fig. 1a.

2) Touchpad configuration: In the touchpad configuration, an inelastic fabric pouch (100 mm × 100 mm × 30 mm) was filled with the particle fluid and secured in a rigid plastic and steel frame, such that the top surface of the pouch was fixed in place with the rest of the pouch and fluid allowed to hang freely. A plastic plate positioned below the pouch is raised or lowered by a DC motor using an elliptical cam with 10 mm of eccentricity. Turning the cam with the motor lifts the plate against the pouch. As the pouch is inelastic, it cannot expand and the particles jam together as they are compressed. This mechanism and the working prototype are shown in Fig. 1b.

## B. Constrictive actuation

In constrictive actuation, a similarly inelastic fabric pouch containing a particle fluid is twisted at one end, with the other end being held in a fixed orientation. This results in the pouch tightening around the fluid, exerting forces inward from all sides. The more the pouch twists, the more force is exerted and the harder the fluid mass becomes.

1) Shaft configuration: In the shaft configuration, a soft, inelastic fabric sleeve (100 mm L × 20 mm dia.) is filled with particles (Quinoa seeds of ~1 mm dia). One end of this sleeve is folded in on itself and clamped between a plastic disc and a rigid frame, such that it cannot move or rotate. The other end is folded and clamped between a plastic disc and a motor shaft coupling, such that it can rotate with the motor shaft. A spring is embedded in the frame to force the ends of the shaft apart when the tension in the fabric is released, loosening the particles. A cross-section of the device construction is shown in Fig. 2a. The finished prototype is fully 3D printed (except for the fabric sleeve) and is also shown in Fig. 2a.

2) Pad configuration: In the pad configuration, a soft fabric pouch (100 mm × 100 mm × 30 mm) is filled with the same particle fluid. This is clamped between a top plate and a rigid support structure, such that the top surface of the pouch is secured in place, with the rest of the pouch allowed to hang down loosely. Four holes in the bottom of the pouch allow the base to be attached to a shaft coupling which is in turn connected to the motor. The motor is fixed to the bottom of the support structure. Turning the motor therefore twists the bottom of the pouch, whilst the top remains fixed in place, causing the sides to tighten around the particle fluid. This mechanical arrangement and finished prototype are shown in Fig. 2b.

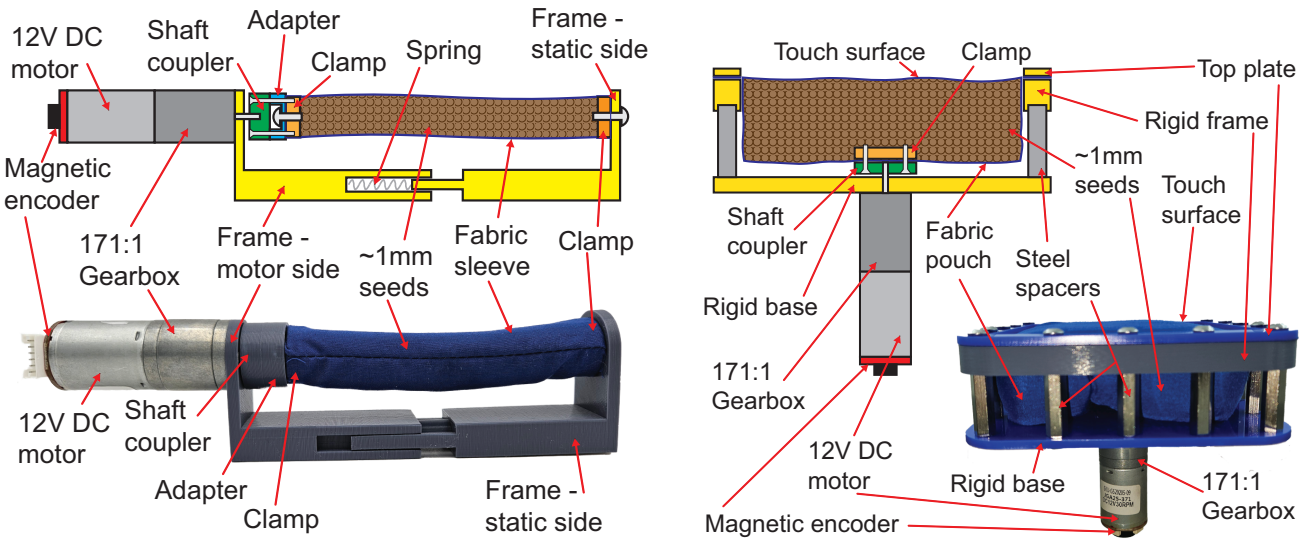


(a) Shaft configuration

(b) Touchpad configuration

Fig. 2: Schematics and prototype devices showing the constrictive actuation technique applied to a) a shaft and b) a touchpad

### C. Control and actuation

All four of the above described devices are driven by 12V brushed DC motors. These motors were fitted with 171:1 reducing gearboxes to increase their torque output and magnetic encoders to enable closed-loop position control for more accurate setting of the device hardness. These were each controlled by an Arduino Uno R3 microcontroller running a customised PID control algorithm at approximately 490Hz via an L298N dual-motor driver chip. For bench testing, desired motor angles were sent to the microcontroller from a PC via the serial port.

## IV. Performance Testing

In order to assess the prototype devices' performance and usefulness, a number of mechanical tests were conducted to characterise their range and uniformity of hardness response, controllability and response time.

### A. Shore Hardness

Shore hardness is a standard measure of material hardness and is based on the indentation of a steel needle under a known force. As hardness-changing haptic interfaces are often used to reproduce the feel of materials of different softness, this is a useful measure of the capabilities of the new devices.

1) Apparatus: The shore hardness evaluation was performed on the touchpad versions of each interface. Each device was raised off the table so that their motors would not collide with the tabletop. A commercially available Shore A Durometer, accurate to $\pm 0.25$, was used to measure the shore hardness of the top surface. The devices were driven by the closed-loop DC motors described in section 3C above. The experiment setup is shown in Fig. 3.

2) Procedure: To measure the shore hardness of each device, both were first set to a neutral position (0°, meaning that the CA pouch was not twisted and the DC eccentric cam was rotated such that it's shortest radius formed a chord with the lift plate). Surface hardness was then measured in 9 locations on the touch surface using the Shore Durometer. The motors were then turned in increments of 10° and 5° for the CA and DC devices respectively, to account for their different ranges of movement. This procedure was repeated three times for each device, and average values computed for surface hardness in each location, at each motor angle.

### B. Flexural Stiffness

Flexural stiffness refers to the ease with which a material will deform when force is applied. It is determined via a standardised test in which a sample with a known thickness or diameter is placed on two rigid supports and a load is applied between them. The deflection of the sample gives an indication of its stiffness. The shaft versions of the two technologies were tested in this way to determine their achievable range of flexural stiffness.

1) Apparatus: The shaft configurations of each mechanism are already fixed at each end, so all that is needed to perform a flexural strength test is a mass, and a means of measuring deflection. For this test, both were achieved by securing a 237g mass to a digital caliper, such that the bottom jaw of the caliper could be fixed to the underside of the support frame, whilst the top jaw was pulled down by the weight and measured the deflection of the sample. This setup is shown in Fig. 4.

2) Procedure: To conduct this test, each sample was attached to the caliper as described above. The caliper was tared to align with the top of the shaft when straight. Each devices' motor was then turned from a neutral

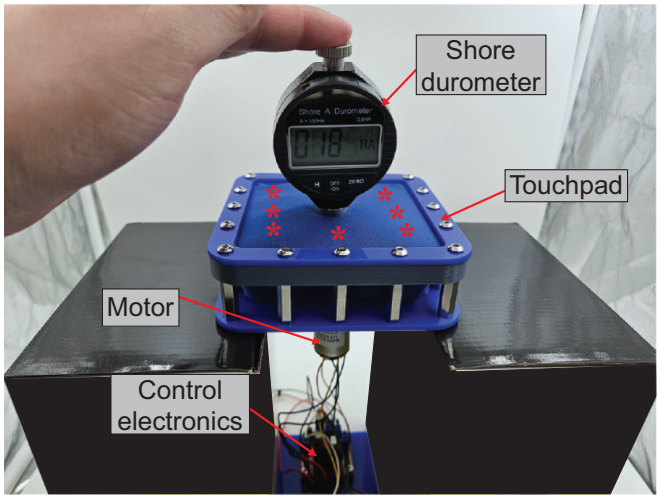


Fig. 3: Apparatus used to measure the shore hardness of the touchpad surface. *s denote the locations hardness measurements were taken.

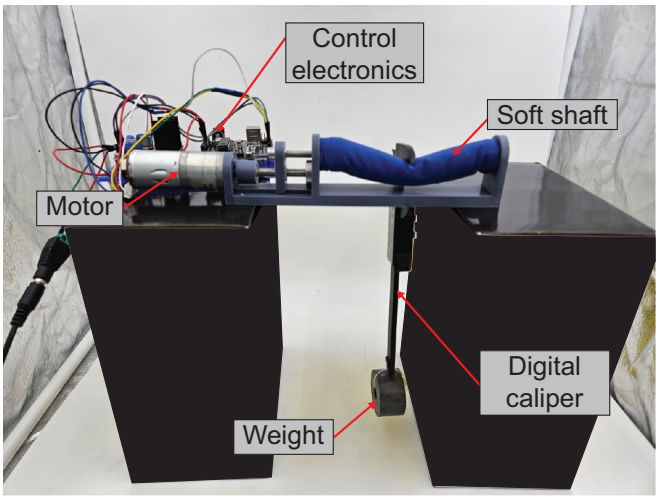


Fig. 4: Apparatus used to measure the flexural stiffness of the shaft prototypes

position (with the CA pouch not twisted and the DC piston fully retracted from the fabric sleeve) to 180°in the case of CA, or 80°in the case of DC, in 10°and 5°increments, respectively. In order to eliminate any possible shape holding effects as shown in [8], [9], the motors were returned to neutral and the weight removed before setting the devices for each measurement. This procedure was repeated three times for each device, and the results averaged.

### C. Response Time

Response time is an important metric for any haptic interface - the faster the mechanical interface can respond to a digital command, the more useful and convincing the feedback will be. The response time of particle jamming-based variable stiffness displays is known to be poor due to the time taken for pressure levels to equalize through what can be large particle volumes and long hose runs. Attempts to improve this through more powerful vacuum sources have been unsuccessful [21].

1) Apparatus: The four prototype variable stiffness devices were set up as they were in previous experiments. The control software for each interface was modified to move from it's minimum and maximum hardness in a single motion, and report the time taken to complete this move.

2) Procedure: In order to measure response time, each variable stiffness interface was programmed to transition from its softest to its hardest state. These states were determined following a brief pilot of the shore hardness and flexural strength tests above, and revealed the following useful ranges of movement:

- CA touchpad: 90°to 160°
- DC touchpad: 2.4 mm to 10 mm
- CA shaft: 50°to 260°
- DC shaft: 2 mm to 13 mm

This process was repeated three times for each interface, with the hardness returned to zero each time. The devices were also shaken slightly between tests to ensure that the particle fluid was soft before each trial. The response times were reported by the motor controller and averages taken to arrive at a final response time value.

## V. Results

### A. Shore Hardness

The shore hardness of the two touchpads was measured under changing motor inputs at various locations across the touch surface. The hardness response in the centre of each touchpad will be presented first, followed by deviations in hardness across each surface.

1) Hardness response: In both devices, the hardness response is generally characterised by two phases. Initially, the motor takes up slack in the pouches such that they are tightened without exerting any noticeable force on the particles. Then, the particles are compressed and become more viscous as they are forced together by each mechanism.

In the constrictive actuation (CA) device, the first half of the range of movement (0°to 90°) showed no appreciable change in hardness (approximately 6A). There was an approximately linear increase in hardness through the next 70°of rotation, with the hardness increasing from 6A to 53A. The final 20°rotation produced a much less pronounced hardness change from 53A to 57A. The test ended here as the motor's rated current was reached.

In the direct compression (DC) device, there was a similar, but shorter, priming phase during the first 2.4 mm of the lifter plate's travel, during which the interface held a consistent 3.5A hardness. The interface then became harder as the plate was lifted further, transitioning approximately linearly from 3.5A to 42.5A

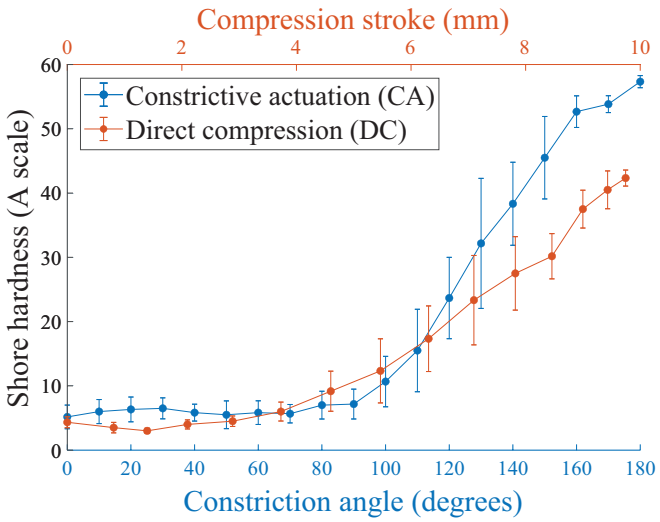


Fig. 5: Shore hardness change measured in the centre of each touchpad, actuated using CA and DC. Error bars represent standard deviation.

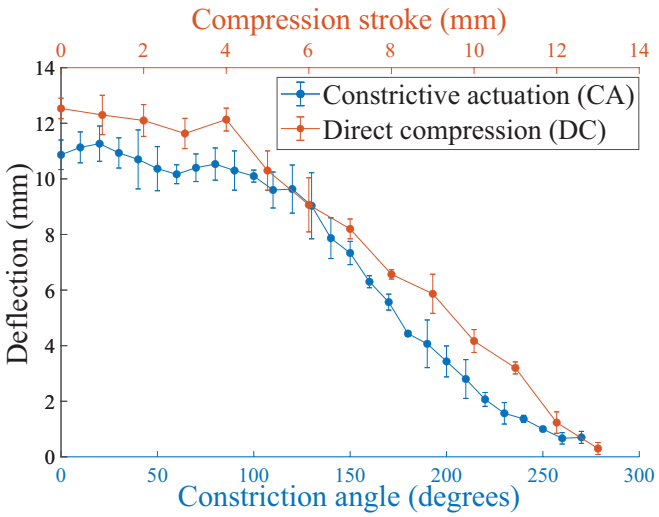


Fig. 7: Deflection under load of the CA and DC based shafts. Error bars represent standard deviation.

until 10 mm of compression was achieved. The test ended here as the motor's current limit was reached.

The hardness responses of both devices are summarised in Fig. 5.

2) Surface uniformity: Measuring different areas of each touchpad revealed a number of differences in how uniform the change in hardness was on each one. In the constrictive actuation (CA) touchpad, the centre was always the hardest part of the surface, with the edges generally being 1-3A softer. The corners were much softer than the centre, generally 4-8A, though deviations of up to 14A from the centre were recorded at the highest stiffnesses. Average hardness deviations are shown graphically in Fig. 6 left.

The direct compression (DC) touchpad was more uniform, with no deviations larger than 5A measured anywhere on the surface during the experiment. The asymmetry across the surface was due to uneven particle loading throughout the volume of the device, an inherent problem with flexible containers. Most measurements were within 2A of each other. The centre was not always the hardest point on the surface. Average hardness deviations are shown graphically in Fig. 6 right.

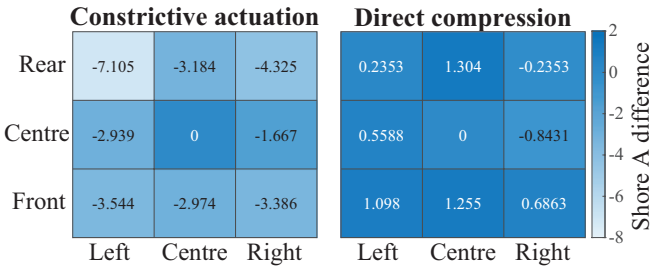


Fig. 6: Average deviation in surface hardness measured on different areas of each touchpad

## B. Flexural stiffness

The flexural stiffness of the two shaft interfaces was recorded as their deflection under identical loads. The constrictive actuation (CA) device was found to show little hardness change during the first 100°of rotation as slack in the fabric was taken up. The deflection under load then decreased almost linearly from a maximum of approximately 10.5 mm in its softest state to a minimum of approximately 0.7 mm in its hardest, at a rotation of 260°. There was then no significant change in hardness during the final 20°of movement. The test ended when the motor current limit was reached.

The direct compression (DC) device was slightly more pliant in its soft state, producing approximately 12.1 mm of deformation during the first 4 mm of compression. The stiffness then increased linearly to a minimum deformation of 0.3 mm after 13 mm of compression. The test ended when the range of movement of the plunger was reached. These results are summarised in Fig. 7.

## C. Response Time

Average response times from the minimum to maximum measured stiffnesses were recorded as follows:

- CA shaft: 1.350 seconds ±0.007
- CA touchpad: 0.741 seconds ±0.006
- DC shaft: 25.367 seconds ±0.170
- DC touchpad: 0.270 seconds ±0.001

# VI. Discussion and Future Work

The results of this performance evaluation show that the constrictive actuation (CA) and direct compression (DC) methods of actuating particle jamming-based haptic interfaces are effective at varying their hardness. Assuming equivalent mechanical power sources, the CA method is able to achieve a greater range of hardness change than the DC approach. Whilst the upper limit of

hardness was lower than has been achieved by pneumatic devices, detailed hardness data has not been published for vacuum actuated jamming interfaces. A scientifically rigorous comparison of achievable hardness change will be performed in a future study. The results for response time were broadly similar to response times observed in vacuum powered particle jamming-based devices (around a second, depending on size/volume [8]). The excessively long response time for the DC shaft was due to the leadscrew mechanism used in the evaluation device, and is not inherent to the jamming effect itself. Response times were, proportional to the movement required to affect each change, suggesting that more powerful motors could adjust the interface hardness faster. The spatial resolution of the display could be increased by arranging jamming pouches in a 2D array, provided that the top surfaces were aligned by way of a rigid frame, similar to the approach used in [12].

The non-pneumatic interfaces demonstrate important practical advantages over vacuum powered approaches to particle jamming-based, hardness-changing displays. Firstly, the size and weight of the actuation systems differ substantially, with a typical vacuum pump (as used in [10]) weighing approximately 6KG, whilst the geared DC motor used in this study weighed 110g, approximately a 98% decrease. This is an important step toward truly portable and wearable variable stiffness haptic interfaces. Secondly, there is a significant difference in cost between the approaches. One unit of the conventional, pneumatic version of the interface would have a total end-user component cost of approximately £400 (vacuum pump: £100; regulator: £270). The non-pneumatic version of the interface has a total material/component cost of approximately £30, based on comparable end-user prices, which is more appropriate for consumer devices.

Future research will investigate how these devices can be incorporated into virtual reality systems to simulate soft objects, as well as adding additional tactile effects, including temperature and texture.

Overall, the approaches explored in this paper demonstrate significant practical benefits over traditional methods of actuating particle jamming-based haptic interfaces. The authors hope that this will encourage more research into hardness-changing haptic interfaces and motivate the soft robotics and soft haptics communities to explore inventive approaches to constructing and controlling soft robotic devices.

## References


[1] M. Mahvash and V. Hayward, "Haptic simulation of a tool in contact with a nonlinear deformable body," in Surgery Simulation and Soft Tissue Modeling, N. Ayache and H. Delingette, Eds. Berlin, Heidelberg: Springer Berlin Heidelberg, 2003, pp. 311–320.

[2] A. Song, J. Liu, and J. Wu, "Softness Haptic Display Device for Human- Computer Interaction," in Human Computer Interaction. InTech, 10 2008.

[3] S. Yoshimoto, Y. Hamada, T. Tokui, T. Suetake, M. Imura, Y. Kuroda, and O. Oshiro, "Haptic canvas: Dilatant fluid based haptic interaction," ACM SIGGRAPH 2010 Emerging Technologies, SIGGRAPH '10, p. 4503, 2010.

[4] Y. Visell, K. A. Duraikkannan, and V. Hayward, "A device and method for multimodal haptic rendering of volumetric stiffness," in Haptics: Neuroscience, Devices, Modeling, and Applications, M. Auvray and C. Duriez, Eds. Berlin, Heidelberg: Springer Berlin Heidelberg, 2014, pp. 478–486.

[5] S. Ullrich and T. Kuhlen, "Haptic Palpation for Medical Simulation in Virtual Environments," Tech. Rep., 2012.

[6] G. Biroli, "A new kind of phase transition?" Nature Physics, vol. 3, pp. 222–223, 2007.

[7] M. van Hecke, "Jamming of soft particles: geometry, mechanics, scaling and isostaticity," Journal of Physics: Condensed Matter, vol. 22, no. 3, p. 033101, 1 2010.

[8] S. Follmer, D. Leithinger, A. Olwal, N. Cheng, and H. Ishii, "Jamming user interfaces: Programmable particle stiffness and sensing for malleable and shape-changing devices," UIST'12, pp. 519–528, 2012.

[9] Y. Kurihara, M. Koge, R. Okazaki, and H. Kajimoto, "Large-area tactile display using vibration transmission of jammed particles," IEEE Haptics Symposium, HAPTICS, vol. 1, no. I, pp. 313–317, 2014.

[10] J. P. Brown and I. Farkhatdinov, "Soft Haptic Interface based on Vibration and Particle Jamming," in IEEE Haptics Symposium, HAPTICS, vol. 2020-March. Washington DC: IEEE, 3 2020, pp. 1–6.

[11] ——, "Using audio recordings to characterise a soft haptic joystick," in Haptic and Audio Interaction Design, C. Saitis, I. Farkhatdinov, and S. Papetti, Eds. Cham: Springer International Publishing, 2022, pp. 102–111.

[12] A. A. Stanley and A. M. Okamura, "Deformable Model-Based Methods for Shape Control of a Haptic Jamming Surface," IEEE Transactions on Visualization and Computer Graphics, 2017.

[13] S. B. Rørvik, M. Auflem, H. Dybvik, and M. Steinert, "Perception by Palpation: Development and Testing of a Haptic Ferrogranular Jamming Surface," Frontiers in Robotics and AI, vol. 8, 9 2021.

[14] T. M. Simon, R. T. Smith, and B. H. Thomas, "Wearable Jamming Mitten for Virtual Environment Haptics," in International Symposium on Wearable Computers. Washington: ACM, 2014, pp. 67–70.

[15] S. Jadhav, M. R. A. Majit, B. Shih, J. P. Schulze, and M. T. Tolley, "Variable Stiffness Devices Using Fiber Jamming for Application in Soft Robotics and Wearable Haptics," Soft Robotics, vol. 9, no. 1, pp. 173–186, 2022.

[16] A. A. Stanley, J. C. Gwilliam, and A. M. Okamura, "Haptic jamming: A deformable geometry, variable stiffness tactile display using pneumatics and particle jamming," 2013 World Haptics Conference, WHC 2013, pp. 25–30, 2013.

[17] A. A. Stanley, D. Mayhew, R. Irwin, and A. M. Okamura, "Integration of a Particle Jamming Tactile Display with a Cable-Driven Parallel Robot," in Haptics: Neuroscience, Devices, Modeling, and Applications, M. Auvray and C. Duriez, Eds. Springer Berlin Heidelberg, 2014, pp. 258–265.

[18] M. Li, T. Ranzani, S. Sareh, L. D. Seneviratne, P. Dasgupta, H. A. Wurdemann, and K. Althoefer, "Multi-Fingered Haptic Palpation utilizing Granular Jamming Stiffness Feedback Actuators Smart Mater," Struct, vol. 23, p. 95007, 2014.

[19] S. J. Estermann, D. H. Pahr, and A. Reisinger, "Quantifying tactile properties of liver tissue, silicone elastomers, and a 3D printed polymer for manufacturing realistic organ models," Journal of the Mechanical Behavior of Biomedical Materials, vol. 104, 4 2020.

[20] T. Sato, J. Pardomuan, Y. Matoba, and H. Koike, "ClaytricSurface: An Interactive Deformable Display with Dynamic Stiffness Control," IEEE Computer Graphics and Applications, vol. 34, no. 3, pp. 59–67, 2014.

[21] I. Zubrycki and G. Granosik, "Novel Haptic Device Using Jamming Principle for Providing Kinaesthetic Feedback in Glove-Based Control Interface," Journal of Intelligent and Robotic Systems: Theory and Applications, vol. 85, no. 3-4, pp. 413–429, 3 2017.